# Combined Experimental and Theoretical Study of Efficient and Ultrafast Energy Transfer in a Molecular Dyad

**ARTICLE** *in* THE JOURNAL OF PHYSICAL CHEMISTRY C · SEPTEMBER 2014

Impact Factor: 4.77 · DOI: 10.1021/jp505957q



**9 AUTHORS**, INCLUDING:

Mariangela Di Donato
University of Florence
**33** PUBLICATIONS **249** CITATIONS
SEE PROFILE

Andrea Lapini
European Laboratory for Non-Linear Spectros…
**23** PUBLICATIONS **115** CITATIONS
SEE PROFILE

Paolo Foggi
Università degli Studi di Perugia
**119** PUBLICATIONS **1,641** CITATIONS
SEE PROFILE

Benedetta Mennucci
Università di Pisa
**249** PUBLICATIONS **24,236** CITATIONS
SEE PROFILE

THE JOURNAL OF PHYSICAL CHEMISTRY C

Article

pubs.acs.org/JPCC

# Combined Experimental and Theoretical Study of Efficient and Ultrafast Energy Transfer in a Molecular Dyad

Mariangela Di Donato,*[,†,‡,§] Alessandro Iagatti,[†,§] Andrea Lapini,[†,‡,§] Paolo Foggi,[†,§,∥] Stefano Cicchi,[‡] Luisa Lascialfari,[‡] Stefano Fedeli,[‡] Stefano Caprasecca,[⊥] and Benedetta Mennucci[⊥]

[†]LENS (European Laboratory for Non Linear Spectroscopy) via N. Carrara 1, 50019 Sesto Fiorentino (FI), Italy

[‡]Dipartimento di Chimica "Ugo Schiff", Universita' di Firenze, via della Lastruccia 13, 50019 Sesto Fiorentino (FI), Italy

[§]INO (Istituto Nazionale di Ottica), Largo Fermi 6, 50125 Firenze, Italy

[∥]Dipartimento di Chimica, Università di Perugia, via Elce di Sotto 8, 06123 Perugia, Italy

[⊥]Dipartimento di Chimica e Chimica Industriale, Università di Pisa, via Risorgimento 35, I-56126 Pisa, Italy

Supporting Information

**ABSTRACT:** We have characterized the dynamics and the efficiency of electronic energy transfer (EET) in a newly synthesized molecular dyad, composed of a styryl-pyridinium donor and a BODIPY acceptor. The kinetics of the process has been studied with femtosecond transient absorption spectroscopy in different solvents. In all the analyzed media EET is quantitative and very fast, as we find that almost 70% of the overall excitation energy is transferred from the donor to the acceptor on a subpicosecond time scale. The experimental measurements have been supported by a theoretical analysis; the electronic couplings between the donor and acceptor moieties have been calculated at the (TD)DFT level and complemented by a conformational analysis of the full dyad. The computed energy transfer times are in good agreement with the experimental values; this allowed us to verify the correctness of the Förster equation, demonstrating that, although EET in the examined system occurs on an ultrafast time scale, the approximations introduced in the case of the weak coupling regime remain valid.

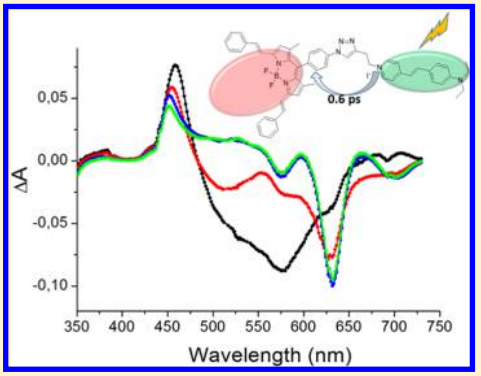


## INTRODUCTION

The increasing demand for clean and renewable energy sources has promoted many attempts at mimicking natural photosynthesis through the development of artificial systems able to efficiently absorb solar light and transform it into useful forms of energy.[1−5] The development of simple molecular arrays able to efficiently transfer the excitation energy among the different units of which they are composed, and to promote charge separation, can be beneficial to disentangle the different molecular and supramolecular factors contributing to the overall energy conversion efficiency.

In natural photosynthesis, sunlight is harvested by specialized protein pigment complexes, the antenna complexes, and the excitation energy is transferred to the reaction center.[6,7] In spite of their structural complexity, due to the presence of a multitude of chromophores with distinct photochemical and photophysical properties embedded in a protein matrix, natural systems have an extremely high energy conversion efficiency. It is clear that a deep understanding of the factors determining the overall efficiency of the photosynthetic machinery is of fundamental importance in order to improve the fabrication of new devices able to convert and store the solar energy.

By using a simplifying approach one must start from a dyad and put attention to the two active parts (donor and acceptor) and also to the nature of the linking scaffold.

In the past few years a large number of studies appeared in the literature, where the properties of this kind of systems were investigated both experimentally and theoretically.[8−11] Among the chromophores commonly used as constituents of artificial photosynthetic systems, $BF_2$-chelated dipyrromethene compounds, usually indicated as BODIPY, have recently attracted attention and have been used both as building blocks of antenna systems and as electron donor or acceptor molecules.[8−13] BODIPY molecules are chemically very stable and possess both high absorption coefficients and high emission quantum yields. Furthermore, their spectral properties can be easily tuned by introducing or varying one or more substituents in the 1−3 and 5−8 positions (Figure 1, left). This nice tunability makes the BODIPY dyes very attractive, since it allows their absorption cross section to be extended over a wide spectral range.[14]

In this work we have synthesized and characterized a bichromophore dyad in which a BODIPY molecule absorbing in the 600 nm spectral range acts as the energy acceptor, while an aminostyrylpyridinium molecule acts as the energy donor. In our system, the two moieties are linked together via a covalent

**Received:** June 16, 2014
**Revised:** September 10, 2014
**Published:** September 18, 2014

   dx.doi.org/10.1021/jp505957q | J. Phys. Chem. C 2014, 118, 23476−23486

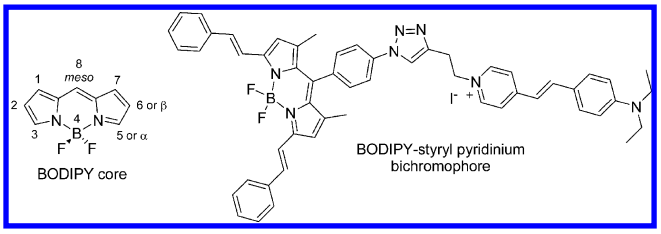


**Figure 1.** Left: BODIPY core. Right: Bichromophore system.

nonconjugated bridge, which should prevent the occurrence of strong excitonic coupling among the two molecular units.

Aminostyrylpyridinium dyes are known heterocyclic organic molecules which have been widely used for several applications. In particular these molecular systems have found applications as laser materials[15,16] or as biological sensors.[17] According to previous studies, their low lying excited state has an intramolecular charge transfer (ICT) character, due to electron density migration from the styryl group to the pyridinium moiety.[18,19] The BODIPY we have chosen has aromatic substituents attached to its core, which shift its absorption and emission spectrum toward the red with respect to the unsubstituted analogue. The structure of the bichromophore is show in Figure 1 (right).

The dynamics of photoinduced energy transfer between the aminostyrylpyridinium donor (D) and the BODIPY acceptor (A) has been studied with transient absorption spectroscopy. As expected, based on the spectral overlap between the donor emission and acceptor absorption spectra, energy transfer in the system is almost quantitative. Furthermore, the process is also extremely fast, we find that 70−80% of the excitation energy is transferred from the donor to the acceptor on a subpicosecond time scale. In order to gain insights into the mechanism of this ultrafast energy transfer we have experimentally analyzed how its kinetics is affected by the external medium, by repeating the measurement in different solvents. The experimental measurements have been complemented by a theoretical analysis based on (TD)DFT computations of the excitonic coupling between the two bichromophore units and a conformational analysis of the whole system in two different solvents.

The kinetics of energy transfer has been analyzed in the frame of Förster theory[20] at room temperature. Despite the ultrafast nature of the process, and the fact that the dipole−dipole approximation overestimates the electronic coupling between the two chromophoric units, we found that the Förster formula is able to reproduce the experimental and calculated rates. The (TD)DFT analysis also allowed us to better clarify this point.

According to our results the kinetics of the process is essentially regulated by the conformational mobility of the system, which allows the two units to come to close contact, thus increasing their spatial overlap and consequently the energy transfer rate. We also show that different solvents can affect the kinetics of energy transfer by modulating the relative stability of different molecular conformations.

## EXPERIMENTAL METHODS

Common reagents were purchased from commercial sources (Sigma-Aldrich and Alfa Aesar) and used without further purification except for the catalyst CuI·P(OEt)$_3$ that was synthesized according to ref 21 but using toluene as solvent instead of benzene. In the following, $R_f$ values refer to TLC on 0.25 mm silica gel plates (Merck F254) obtained using the same eluent as in the separation of the compound by flash column chromatography. If not otherwise specified, the stationary phase is always silica. $^1$HNMR spectra were recorded with Varian Gemini apparatus. Chemical shift values are expressed in $\delta$(ppm) with respect to the tetramethylsilane (TMS) resonating frequency. Notations s, d, t, q, m, and p (and their combinations), refer to signal multiplicity and mean singlet, triplet, quartet, multiplet, and pseudo. Mass spectra were recorded with a LCQ-Fleet Thermo Scientific Electron Spray Ionization (ESI-MS) apparatus. Intensities are reported in $m/z$, and the intensity is expressed as a percentage with respect to the most intense peak.

**Scheme 1. Synthesis of the Bichromophore**

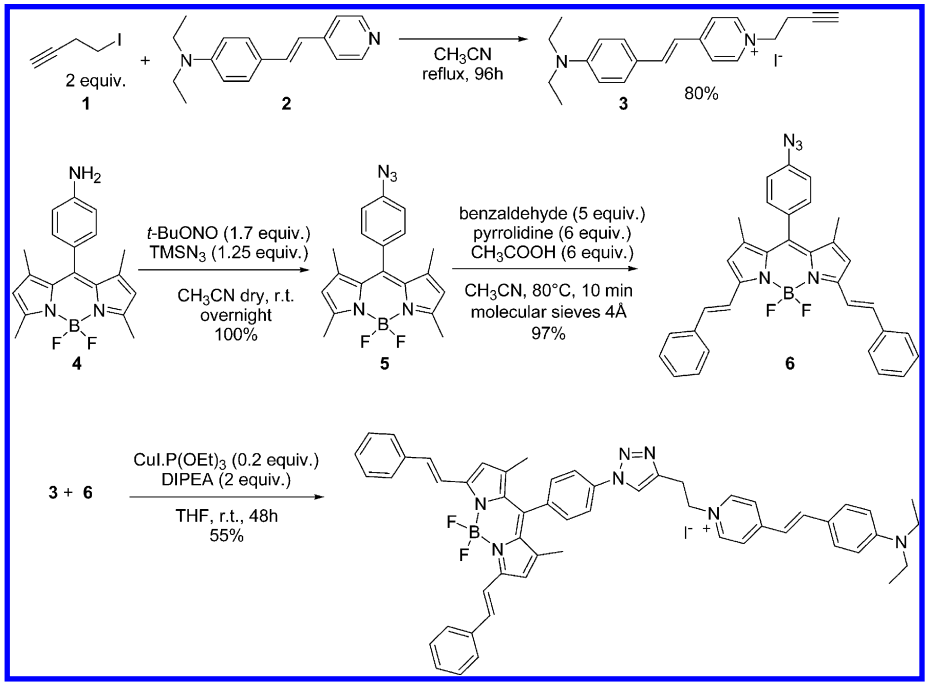



dx.doi.org/10.1021/jp505957q | J. Phys. Chem. C 2014, 118, 23476−23486

IR spectra were recorded using a PerkinElmer FR-IR 881 spectrometer, absorption bands are expressed by wavenumbers ($cm^{-1}$). Notations w, m, and s, referring to the signal intensity, are weak, medium, and strong. UV−visible spectra were recorded using a Varian Cary 4000 UV−vis spectrophotometer or a PerkinElmer Lambda 950 spectrometer. Fluorescence spectra were recorded using a Jasco FP-750 spectrofluorimeter, and absorption and emission peaks are listed. Fluorescence quantum yields were obtained by measuring the corrected area of samples and standards: Rhodamine 6G ($\Phi = 0.94$)[22] for the donor and Cresyl violet ($\Phi = 0.56$)[23] for both the acceptor and the bichromophore. Elemental analysis were performed with PerkinElmer 240 instrumentation.

**Synthetic Procedure.** The synthesis of the bichromophore was realized according to Scheme 1. Compounds **1** and **2** were synthesized accordingly to refs 24 and 25, respectively. Compound **4** was derived from its nitro precursor following already reported literature procedures [For the synthesis of nitroprecursor of **4**, see ref 26; for the reduction of the nitro group to amine for the obtainment of **4**, see ref 27].

Synthesis of 1-but-3-ynyl-4-[2-(4-diethylamino-phenyl)-vinyl]-pyridinium iodide (**3**). Iodide **1** (240 mg, 1.33 mmol) and 4-[2-[4-(diethylamino)phenyl]ethenyl]-pyridine **2** (168 mg, 0.67 mmol) were dissolved in anhydrous $CH_3CN$ (12 mL). The mixture was refluxed under $N_2$ atmosphere. The reaction was monitored by TLC ($CH_2Cl_2$/MeOH 10:1, $R_f = 0.38$). After 96 h the solvent was evaporated and the reaction product was purified by flash chromatography, eluting first with $CH_2Cl_2$/MeOH 50:1 and then $CH_2Cl_2$/MeOH 25:1, to afford compound **3** (232 mg, 80% yield). $^1$HNMR (300 MHz, $CDCl_3$): $\delta = 8.85$ (d, $^3J = 6.9$ Hz, 2H), 7.82 (d, $^3J = 6.9$ Hz, 2H), 7.63 (d, $^3J_{trans} = 15.9$ Hz, 1H), 7.53 (d, $^3J = 9.0$ Hz, 2H), 6.85 (d, $^3J_{trans} = 15.9$ Hz, 1H), 6.64 (d, $^3J = 9.0$ Hz, 2H), 4.79 (t, $^3J = 6.0$ Hz, 2H), 3.41 (q, $^3J = 7.2$ Hz, 4H), 2.95 (td, $^3J = 6.0$ Hz, $^4J = 2.7$ Hz, 2H), 2.12 (t, $^4J = 2.7$ Hz, 1H), 1.19 (t, $^3J = 7.2$ Hz, 6H) ppm; UV−vis ($CH_2Cl_2$) $\lambda_{max} = 533$ nm; Fluorescence ($CH_2Cl_2$) $\lambda_{max} = 608$ nm; MS (ESI): $m/z$ (%) = 305.24 (100) $[M\text{-}I^-]^+$, 732.52 (14) $[M+(M\text{-}I^-)]^+$; Elemental analysis calcd for $C_{21}H_{25}IN_2$: N 6.48, C 58.34, H 5.83; found N 6.08, C 57.97, H 5.89.

Synthesis of 4,4-difluoro-8-(4-azidophenyl)-1,3,5,7-tetramethyl-4-bora-3a,4a-diaza-*s*-indacene (**5**). The amino-Bodipy **4** (177 mg, 0.5 mmol) was dissolved in anhydrous $CH_3CN$ (10 mL). The resulting solution was cooled at 0 °C; then *tert*-butyl nitrite (0.1 mL, 0.84 mmol, 1.7 equiv) and trimethylsilyl azide (82 μL, 0.625 mmol, 1.25 equiv) were added. The reaction mixture was allowed to return to r.t. and was stirred overnight under inert atmosphere. The solution was then concentrated to give the desired product in quantitative yield. $^1$HNMR (200 MHz, $CDCl_3$): $\delta = 7.28$ (AA′-BB′ system, $J = 8.0$ Hz, 2H), 7.17 (AA′-BB′ system, $J = 8.0$ Hz, 2H), 5.98 (s, 2H), 2.55 (s, 6H), 1.41 (s, 6H) ppm; UV−vis (DMF): 502 nm; Fluorescence (DMF): 514 nm. For full characterization see ref 28.

Synthesis of **6**. Compound **5** (88 mg, 0.25 mmol) was dissolved in anhydrous $CH_3CN$ (12 mL), and then 4 Å molecular sieves were quickly introduced in the reaction vessel. Then benzaldehyde (130 μL, 1.28 mmol, 5 equiv), pyrrolidine (125 μL, 1.50 mmol, 6 equiv) and glacial acetic acid (85 μL, 1.50 mmol, 6 equiv) were added. The reaction was immersed in a 80 °C preheated oil bath and in few minutes the color turned from red to a dark blue. The reaction was monitored by TLC until the complete formation of the product occurred ($CH_2Cl_2$/Et.p 1:1 $R_f = 0.53$). After less than 30 min the reaction was completed, and the mixture was allowed to cool to r.t. and then $CH_2Cl_2/Et_2O$ (1:2) was added. The organic layer was subsequently washed with HCl (0.05 M, 40 mL ×2), with saturated $NaHCO_3$ (20 mL) and with brine (20 mL). The organic layer was dried over $Na_2SO_4$ and then reduced to dryness to give **6** (127 mg, 97%) that was employed without further purification. $^1$HNMR (400 MHz, $CDCl_3$): $\delta = 7.74$ (d, $^3J_{trans} = 16.4$ Hz, 2H), 7.64 (d, $^3J = 7.6$ Hz, 4H), 7.41 (pt, 4H), 7.33 (m, 4H), 7.26 (d, $^3J_{trans} = 16.4$ Hz, 2H), 7.18 (d, $J = 8.4$ Hz, 2H), 6.66 (s, 2H), 1.50 (s, 6H) ppm; $^{13}$CNMR (100 MHz, $CDCl_3$): $\delta = 152.8$ (s), 141.9 (s), 141.1 (d), 137.9 (s), 136.5 (d), 136.4 (d), 133.4 (s), 131.7 (s), 130.1 (d), 129.0 (d), 128.8 (d), 127.6 (d), 119.7 (d), 119.2 (s), 117.9 (s), 14.9 (q) ppm; UV−vis ($CH_2Cl_2$) $\lambda_{max} = 347$ nm, 577 nm, 626 nm; Fluorescence ($CH_2Cl_2$) $\lambda_{max} = 640$ nm; IR ($CDCl_3$): $\nu = 3063$ (w), 2930 (w), 2127 (m), 2108 (m), 1618 (m), 1539 (s), 1500 (s), 1494 (s), 1446 (m), 1371 (m), 1298 (m), 1200 (s), 1150 (s) $cm^{-1}$. Anal. Calcd for $C_{33}H_{26}N_5BF_2$: N, 12.94; C, 73.21; H, 4.84. Found: C, 12.80; N, 73.39; H, 4.98.

Synthesis of bichromophore. Compounds **6** (126 mg, 0.23 mmol) and **3** (124 mg, 0.29 mmol, 1.25 equiv) were dissolved in anhydrous THF (5 mL). Then *N*,*N*-diisopropylethylamine (81.1 μL, 60.2 mg, 0.46 mmol, 2 equiv), and CuI·P(OEt)$_3$ (28 mg, 0.08 mmol, 0.3 equiv) were added. The mixture was stirred at r.t. in $N_2$ atmosphere for 72 h, and it was monitored by TLC ($CH_2Cl_2$/MeOH 10:1). Then the solvent was evaporated, and the crude was purified by flash chromatography on alumina (activity V, pH 7) eluting with $CH_2Cl_2$/MeOH 50:1 ($R_f = 0.22$) to give the product as a dark powder (126 mg, 55% yield). $^1$HNMR (400 MHz, $CDCl_3$): $\delta = 9.03$ (s, 1H), 9.01 (2H, $^3J = 6.8$ Hz, 2H), 8.04 (2H, $^3J = 8.4$ Hz, 2H), 7.73 (d, $^3J_{trans} = 16.4$ Hz, 2H), 7.68 (d, $^3J = 6.8$ Hz, 2H), 7.65 (d, $^3J = 7.2$ Hz, 4H), 7.54 (d, $^3J_{trans} = 15.6$ Hz, 1H), 7.49 (pd, 4H), 7.40 (pt, 4H), 7.32 (m, 4H), 6.77 (d, $^3J_{trans} = 15.6$ Hz, 1H), 6.67 (pt = s + d, 4H), 5.13 (t, $^3J = 7.0$ Hz, 2H), 3.70 (t, $^3J = 7.0$ Hz, 2H), 3.43 (q, $^3J = 7.1$ Hz, 4H), 1.49 (s, 6H), 1.22 (t, $^3J = 7.1$ Hz, 6H) ppm; $^{13}$CNMR (100 MHz, $CDCl_3$): $\delta = 154.6$ (s), 153.0 (s), 150.5 (s), 143.6 (s), 143.2 (d), 142.7 (s), 142.0 (d), 137.4 (s), 137.1 (s), 136.6 (d), 136.5 (d), 133.2 (d), 131.2 (d), 130.2 (d), 129.0 (d), 128.8 (d), 127.6 (d), 122.8 (s), 122.1 (d), 121.4 (s), 120.9 (d), 119.2 (s), 118.1 (d), 115.4 (d), 111.6 (d), 58.4 (t), 44.7 (t), 27.7 (t), 15.1 (q), 12.6 (q) ppm; UV−vis ($CH_2Cl_2$) $\lambda_{max} = 350$ nm, 533 nm, 574 nm, 628 nm; Fluorescence ($CH_2Cl_2$) $\lambda_{max} = 643$ nm; IR ($CDCl_3$): $\nu = 3005$ (w), 2974 (w), 2930 (w), 1710 (s), 1574 (s), 1541 (m), 1524 (s), 1508 (m), 1439 (m), 1411 (m), 1364 (s), 1325 (w), 1223 (m), 1164 (m), 1153 (m) $cm^{-1}$; MS (ESI): $m/z$ (%) = 846.47 (100) $[M\text{-}I^-]^+$.

**Transient Absorption Measurements.** The apparatus used for the transient absorption spectroscopy (TAS) measurements has been described in detail in previous works.[29−32] The fs-laser oscillator is a Ti:sapphire laser (Spectra Physics Tsunami) pumped by the second harmonic of a Nd:YVO (Spectra Physics Millennia). The short (≤70 fs) pulses are stretched and amplified at 1 kHz repetition rate by a regenerative amplifier (BMI Alpha 1000). After compression a total average power of 450−500 mW and pulse duration of 100 fs are obtained. The repetition rate of the output beam is reduced to 100 Hz by a mechanical chopper in order to avoid the photodegradation of the sample. Pulses in the UV−visible range can be achieved by second harmonic generation (SHG) or by doubling or mixing the output of an optical parametric generator and amplifier (OPG-OPA) based on a BBO crystal (TOPAS by Light Conversion, Vilnius, Lithuania).[33,34] For the current measurements the pump beam polarization was set to magic angle with respect to the probe beam by rotating a $\lambda/2$ plate so as to exclude


dx.doi.org/10.1021/jp505957q | J. Phys. Chem. C 2014, 118, 23476−23486

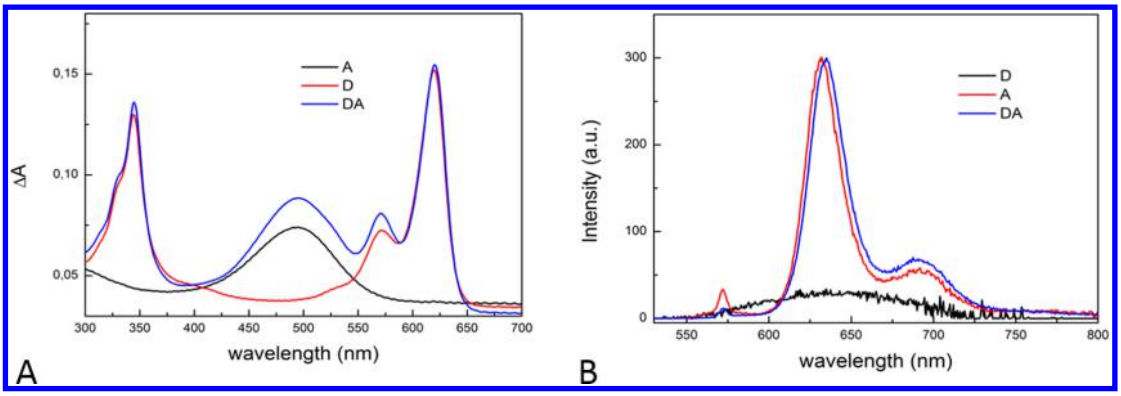


**Figure 2.** Steady state (A) absorption and (B) fluorescence spectra of the aminostyrylpyridinium donor (black line), the BODIPY acceptor (red line) and the D−A dyad (blue line) in acetonitrile. The fluorescence spectrum of the bichromophore is registered upon excitation at 500 nm, that of the acceptor upon excitation at 570 nm.

rotational contributions to the transient signal. The probe pulse was generated by focusing a small portion of the 800 nm radiation on a 3 mm thick $CaF_2$ window mounted on a motorized translation stage. The continuum light was optimized for the 350−750 nm wavelength range, and a moveable delay line made it possible to increase the time-of-arrival-difference of the pump and probe beams up to 2.0 ns. Multichannel detection for transient spectroscopy was achieved by sending the white light continuum after passing through the sample to a flat field monochromator coupled to a homemade CCD detector [http://lens.unifi.it/ew]. TAS measurements were carried out in a static cell (2 mm thick) under magnetic stirring in order to refresh the solution and avoid photo degradation.

The integrity of the sample has been checked by visible absorption measurements (PerkinElmer LAMBDA 950) before and after the time-resolved measurements. The OD of the sample at the excitation wavelength was between 0.2 and 0.5 in all the examined solvents (chloroform, acetonitrile, and benzonitrile).

**Data Analysis.** Transient spectra have been analyzed by applying a combined approach, consisting of singular values decomposition (SVD)[35−37] and the simultaneous fitting of all the collected kinetic traces (global analysis). The aim of global analysis is to decompose the two way data matrix into time-independent spectra and wavelength independent kinetics.[38] Once the number of components is identified through the SVD, the second step involves the parametrization of the time evolution of the spectral components. This was accomplished by assuming first-order kinetics, describing the overall temporal evolution as the sum or combination of exponential functions. Global analysis was performed using the GLOTARAN package (http://glotaran.org)[38,39] and employing a linear unidirectional "sequential" model.

**Computational Strategy.** The computational analysis has been based on a (TD)DFT description of the geometries and electronic properties of the system, with the effect of the environment included through the polarizable continuum model (PCM).[40] Within this framework, the QM D−A pair is embedded in a cavity of shape and dimension defined according to the geometrical structure of the molecules and their relative orientation and distance. The solvent is described as a polarizable continuum (characterized by its dielectric constant and refractive index), which responds to the presence of the QM system through a set of induced (or apparent) charges appearing on the surface of the molecular cavity. In turn, such charges act back on the QM system from which they are generated: this mutual polarization effect is solved through a modified self-consistent field scheme. In addition, within the PCM framework it is possible to introduce nonequilibrium effects that appear any time a fast process in the QM system originates delays in the response of the solvent. This is exactly what happens during an electronic excitation followed by an electronic energy transfer (EET) process. In the common time-scales of these processes, the response of the solvent is incomplete in the sense that only its fast degrees of freedom (of electronic nature) can equilibrate with the final state of the QM system, while the rest remains frozen in the initial configuration corresponding to the QM system before the change.

The excitonic coupling between two units $i$ and $j$ is calculated using a perturbative approach from the transition densities of the noninteracting units, $\tilde{\rho}_{i,j}$. In the case of systems in vacuo, the coupling is composed of three terms, referred to as Coulomb, exchange-correlation, and overlap coupling terms, respectively[41]

$$V_{ij} = \int \mathrm{d}\vec{\mathbf{r}}\, \mathrm{d}\vec{\mathbf{r}}' \tilde{\rho}_i(\vec{\mathbf{r}}) \frac{1}{|\vec{\mathbf{r}} - \vec{\mathbf{r}}'|} \tilde{\rho}_j(\vec{\mathbf{r}}') + \int \mathrm{d}\vec{\mathbf{r}}\, \mathrm{d}\vec{\mathbf{r}}' \tilde{\rho}_i(\vec{\mathbf{r}}) g_{\mathrm{xc}} \tilde{\rho}_j(\vec{\mathbf{r}}') - \omega \int \mathrm{d}\vec{\mathbf{r}}' \tilde{\rho}_i(\vec{\mathbf{r}}) \tilde{\rho}_j(\vec{\mathbf{r}}) \quad (1)$$

In the last equation, the first term on the right is the Coulomb contribution and has a physical correspondence with the classical point-dipole/point-dipole interaction term, while $g_{\mathrm{xc}}$ is a general exchange-correlation kernel, determined by the choice of functional used in the (TD)DFT scheme. The last term is an overlap contribution weighted by the resonance transition energy $\omega$. Equation 1 was originally derived for the resonant case; we have extended it to the more general case where the chromophores' excitation energies are not identical, by using an average value of $\omega$; we note however that the overlap term is practically negligible, if compared to the other ones.

Within the PCM framework, the solvent effect enters in the definition of the coupling through an additional term to be added to the equation (1). Namely, if we mimic the solvent polarization induced by the donor transition densities in terms of PCM charges, such an additional term, $V_{\mathrm{PCM}}$, describes the interaction between the transition density of the unit $i$ with the PCM charges induced by the other unit $j$, namely:[42]

$$V_{\mathrm{PCM}} = -\sum_t \left[ \int \mathrm{d}\vec{r}\ \tilde{\rho}_i(\vec{r}) \frac{1}{|\vec{r} - \vec{r}_t|} \right] q_t(\varepsilon_\infty; \tilde{\rho}_j) \quad (2)$$


dx.doi.org/10.1021/jp505957q | J. Phys. Chem. C 2014, 118, 23476−23486

where a nonequilibrium response for the environment (indicated by the dynamic or optical part of the permittivity, $\varepsilon_\infty$, i.e. the square of the refractive index) is used.

All the calculations have been performed with a locally modified version of the Gaussian 09 suite of programs.[43] The ground state geometries have been optimized in the proper solvent using the M06-2X[44] level of theory with the 6-311G(d) basis set; the same approach has been used for the conformational analysis. Transition energies, transition densities, and couplings have been computed at (TD)DFT level using the CAM-B3LYP[45] functional in combination with the 6-311+G-(2d,p) basis set. In this study the solvent is introduced using the integral equation formalism[46] version of PCM (IEFPCM). Cavities were built using the united atom topological model and the IEFPCM calculations were performed with G03default option.

## RESULTS

**Steady-State Measurements.** The absorption and emission spectrum of the donor (D), acceptor (A), and bichromophore dyad (D−A) are reported in Figure 2. The absorption spectrum of the bichromophore can be almost exactly reproduced by the sum of the two independent moieties, which is indicative for a small electronic coupling between the donor and acceptor molecules. The emission of the donor and the absorption of the acceptor have a good spectral overlap, which is a prerequisite for an efficient excitation energy transfer (EET). Furthermore, the high Stokes shift between the absorption and emission spectra of the donor reduces potential autoabsorption phenomena. On the contrary only a modest Stokes shift is observed for the acceptor, as typical for BODIPY dyes. The emission of the D−A system is essentially identical to that of the isolated acceptor; in acetonitrile it is centered at 632 nm with a shoulder at 692 nm. The residual donor emission cannot be detected, indicating efficient energy transfer.

The fluorescence quantum yields (QY) measured for the molecules under investigation, using Rhodamine 6G and Cresyl violet as standards, are reported in Table 1. The donor has a very low QY with values ranging from 0.1 in chloroform to only 0.005 in acetonitrile, suggesting the presence of efficient nonradiative deactivation pathways. On the contrary the acceptor has a quite high QY in all the examined solvents, as it is known for BODIPY dyes.[14] The dyad has also a significant QY, comparable to that of the isolated acceptor when excited on the acceptor moiety in both chloroform and benzonitrile, but reduced by a factor 2 in acetonitrile. Significant fluorescence QY is also observed in the dyad when excited on the donor moiety, despite the low QY of the isolated donor, suggesting the occurrence of efficient EET.

**Table 1. Fluorescence QY of Donor, Acceptor, and D−A Dyad in Chloroform, Acetonitrile and, Benzonitrile**

| | $\phi$ ($\lambda_{exc}$) |
|---|---|
| | Donor |
| chloroform | 0.1 (530 nm) |
| acetonitrile | 0.005 (530 nm) |
| benzonitrile | 0.09 (530 nm) |
| | Acceptor |
| chloroform | 0.8 (620 nm) |
| acetonitrile | 0.65 (620 nm) |
| benzonitrile | 0.87 (620 nm) |
| | Dyad |
| chloroform | 0.78 (620 nm); 0.38 (500 nm) |
| acetonitrile | 0.35 (620 nm); 0.16 (500 nm) |
| benzonitrile | 0.87 (620 nm); 0.37 (500 nm) |

**Ultrafast Transient Absorption Measurements.** The excited state evolution of the systems under investigation and the kinetics of EET in the bichromophore were analyzed by means of transient absorption spectroscopy in the visible spectral range. Before the analysis of the dyad, we have studied the donor and acceptor systems separately in order to characterize their typical transient absorption bands and analyze if their photophysical properties are modified in the dyad.

*Donor and Acceptor Moieties.* Transient spectra of both the donor and acceptor moieties have been collected in chloroform and acetonitrile. Excitation of the donor species was obtained by pumping the molecule at 520 nm, while for the acceptor the excitation wavelength has been set at 570 nm. Since the excitation beam is tuned at wavelength near the absorption maximum of the donor, the bleaching signal is not well resolved due to the scattered light of the pump. In order to extract information on the dynamic evolution of the photoexcited systems, the kinetic traces of both the donor and acceptor were globally analyzed, using a sequential kinetic scheme with increasing lifetimes. The Evolution Associated Decay Spectra (EADS) obtained for the donor and acceptor molecules in chloroform are shown in Figure 3, the data recorded in acetonitrile are reported in the Supporting Information.

In case of the donor four kinetic constants were necessary to obtain a satisfactory fit of the data, while only three constants were sufficient for the acceptor data. Looking at the donor EADS it is possible to identify an excited state absorption (ESA) band centered at 450 nm and a stimulated emission (SE) band initially peaked at 570 nm, evolving toward longer wavelengths on a few picosecond time scale (black to red and red to blue EADS evolution). The red shift of the stimulated emission is ascribable to a dynamic Stokes shift, induced by the reorganization of the solvent around the sample in the excited state. This process is particularly evident for this molecule, and it can be well explained in the frame of the proposed excited state evolution scheme of the styryl-pyridinium molecule. In fact it has been shown that for this class of molecules an excited state with partial intramolecular charge transfer (ICT) is formed upon photoexcitation, in which the charge is transferred from the styryl to the pyridinium group.[19] The significant dipole moment variation associated with the charge transfer process justifies the observation of this relevant Stokes shift, which evolves biexponentially and is completed within 1.6 ps. The excited state population mostly decays with a 254 ps lifetime, thus justifying the low fluorescence QY measured for this system, although a longer 1 ns lifetime is found, only associated with a small residual bleach signal. The sample behaves very similarly in acetonitrile, see spectra and analysis in the SI. Transient bands are narrower in this solvent and slightly red-shifted. Again, fast dynamic Stokes shift is observed, but in this case an even faster ground state recovery is retrieved. Here in fact the system relaxes within 25 ps suggesting the presence of a larger contribution of nonradiative deactivation pathways.

The EADS of the acceptor molecule, reported in Figure 3B in chloroform, shows the typical evolution of a BODIPY system.[14] Soon after excitation (black EADS with 400 fs lifetime) an intense stimulated emission band is observed, peaked at 635 nm in chloroform (625 nm acetonitrile, see the SI). The bleaching band is almost contained in the SE band, due to the small Stokes shift of the BODIPY emission with respect to its absorption.


dx.doi.org/10.1021/jp505957q | J. Phys. Chem. C 2014, 118, 23476−23486

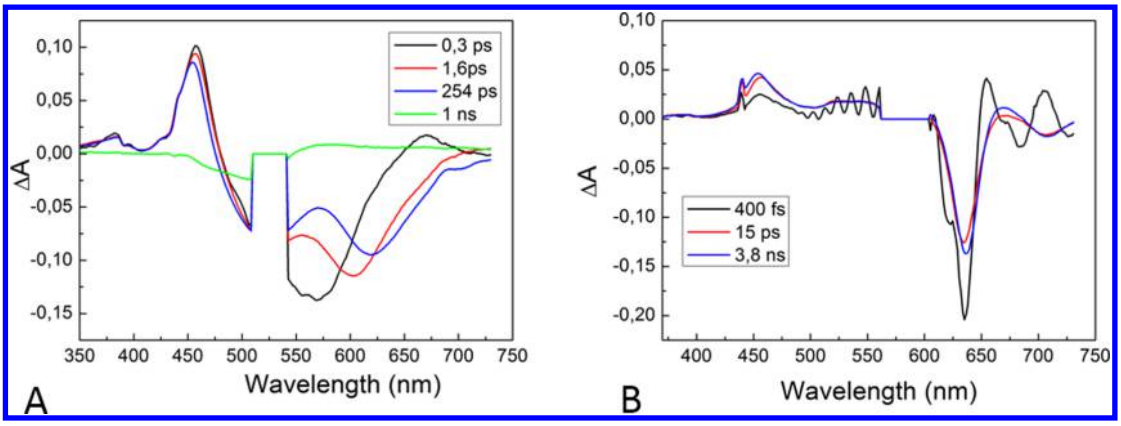


**Figure 3.** EADS obtained from global analysis of time-resolved data for the donor (panel A) and the acceptor (panel B) molecules measured in chloroform.

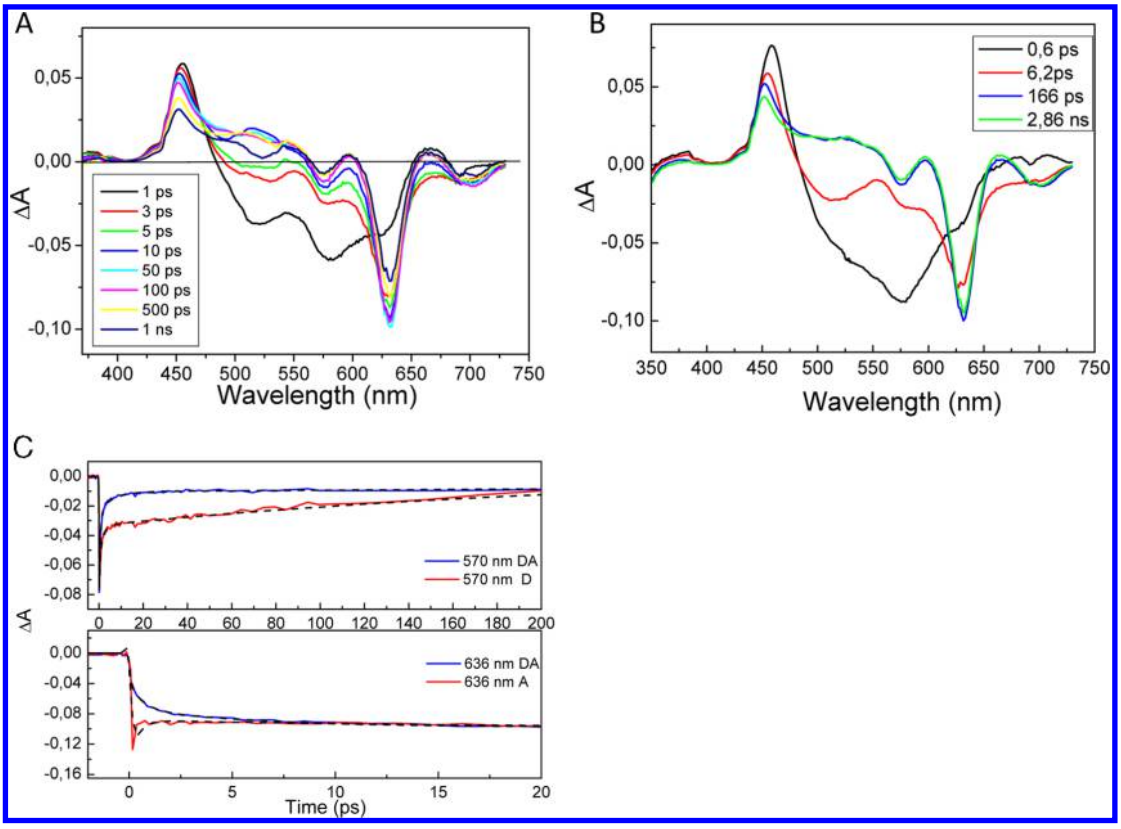


**Figure 4.** (A) Selected transient spectra of the D−A dyad measured in chloroform (uncorrected for dispersion of the white light probe); (B) EADS obtained from global analysis of the transient data of the bichromophore in chloroform; (C) comparison between significant kinetic traces of the isolated donor (red line) and the D−A system (blue line, upper panel) together with the fit from global analysis (dotted lines). In the lower panel of the same figure kinetic traces are reported for the isolated acceptor (red line) and the D−A system (blue line) together with the fit from global analysis (dotted lines).

Besides the SE band, the transient spectra also show an ESA band peaked around 455 nm, which slightly blue shifts on a 15 ps time scale (red to blue EADS evolution). The dynamic evolution of the system is very limited, and no significant shifts or band-shape variation are observed for both the SE and ESA bands. The system decays with a rather long 3.8 ns lifetime (3.4 in ACN), which justifies the observed high fluorescence QY. The photodynamics of this system is not affected by the solvent, so both the transient spectra and their evolution are very similar in acetonitrile with respect to those measured in chloroform.

*Bichromophore Dyad.* Transient spectra of the bichomophore system have been recorded by exciting the sample on the donor moiety, at 530 nm. At this wavelength the absorption of the acceptor is negligible, which minimizes its direct excitation. Besides chloroform and acetonitrile transient spectra have been recorded in this case also in benzonitrile, in order to better characterize how the different environments can affect the kinetics of energy transfer. Selected transient spectra recorded in chloroform and the EADS obtained by the global analysis are reported in Figure 4, and the data analysis for the two other investigated solvents are reported in the SI. In Figure 4 we also report the comparison between selected transient absorption traces recorded for the bichromophore dyad with the


dx.doi.org/10.1021/jp505957q | J. Phys. Chem. C 2014, 118, 23476−23486

corresponding traces measured for the isolated donor and acceptor, highlighting the occurrence of energy transfer.

At early delay times after excitation, the transient spectra reported in Figure 4 show characteristic signals both of the donor and acceptor moieties. The SE band centered around 575 nm is ascribable to the donor and disappears almost completely on a few picoseconds time scale. The longer wavelength negative band, centered at ca. 630 nm is due to a combination of the bleaching and SE of the BODIPY acceptor. This signal appears in the transient spectra on a subpicosecond time scale, indicating the occurrence of fast energy transfer in the system. The ESA centered around 450 nm is a convolution of the signals of the two isolated moieties, since both the reference compounds have similar signals in that spectral region. The comparison of the transient traces measured for the isolated D and A moieties with those of the bichromophore shows significant differences at early delay times, ascribable to the occurrence of energy transfer. In particular, the 570 nm time trace of the bichromophore, in the region of the donor stimulated emission, decays faster than in the isolated donor, while the trace at 636 nm, due to the acceptor stimulated emission has a slower rise component with respect to the isolated acceptor molecule.

The dynamic evolution of the dyad is better visualized by inspecting the EADS obtained by global analysis. The good quality of the fit is testified by a very low value of the root-mean-square error (RMS), which is on the order of 0.001, and the agreement between the fit and the kinetic traces reported in Figure 4. In the first EADS, black line in Figure 4B, the bleaching/SE signals of the donor are well evident. Notice that in the 470−600 nm region this EADS clearly recalls the first component obtained for the isolated donor (see Figure 3A). This component decays in ca. 600 fs in the second EADS, where only a significantly smaller donor signal is observed, while the SE of the acceptor, centered at 630 nm, is already well evident. This evolution indicates that at least 70% of the energy transfer occurs on a subpicosecond time scale. The second EADS decays within 6.2 ps in the third spectral component (green line), which already closely recalls the transient spectra of the isolated acceptor, thus showing the occurrence of quantitative energy transfer. The last spectral component, which is formed in 166 ps and decays in 2.8 ns is substantially similar to the long time component of the isolated acceptor. Only a modest spectral evolution is observed on the 166 ps time scale; however, the inclusion of this kinetic component in the analysis is necessary in order to correctly fit the kinetic traces on the longer nanosecond time scale. The analysis of the EADS thus suggests the occurrence of quantitative energy transfer in the system, occurring for almost 70% on a subpicosecond time scale. Although energy transfer appears to occur with multiexponential kinetics, more than 95% of the energy is on the acceptor moiety in less than 10 ps. The transient spectra obtained in the two other analyzed solvents are qualitatively similar to those measured in chloroform. However, the kinetics of energy transfer changes to some extent depending on the environment. While comparatively even faster kinetics are observed in acetonitrile, where almost 80% of energy transfer occurs in 300 fs, the process is slower in benzonitrile. The kinetic parameters obtained for the three analyzed solvents are reported in Table 2.

The longer lifetime, which should be similar to that of the isolated acceptor (ca. 3.8 ns) is shortened in the bichromophore both in chloroform and acetonitrile, while it does not change in benzonitrile.

**Table 2. Lifetimes Obtained from Global Analysis of the Time Resolved Data of the D-A Dyad in the Three Analyzed Solvents**

| solvent | $t_1$ (ps) | $t_2$ (ps) | $t_3$ (ps) | $t_4$ (ns) |
|---|---|---|---|---|
| Chloroform | 0.6 | 6.2 | 166 | 2.86 |
| Acetonitrile | 0.26 | 5.5 | 33 | 2.1 |
| Benzonitrile | 1.7 | 10.0 | 478 | 3.9 |

This finding could be related to the different viscosity of the used solvents (chloroform: 0.7; acetonitrile: 035; benzonitrile: 1.4). Viscosity in fact slows down the internal rotation thus reducing the activity of additional nonradiative decay channels. The occurrence of strong excitonic coupling between the two moieties, which could in principle promote retro-donation of the excitation energy, has been ruled out by performing transient absorption measurements on the bichromophore setting the excitation wavelength on the acceptor (at 610 nm). The obtained transient spectra are reported in the SI, where it is shown that the signal closely recalls that of the isolated acceptor for the entirely explored time window, and no spectral signatures attributable to the donor are observed.

**Computational Results.** The EET rate between a molecular pair of donor D and acceptor A is here obtained in the weak-coupling limit, by applying the Fermi golden rule

$$k^{\mathrm{EET}} = \frac{2\pi}{\hbar} V^2 J \tag{3}$$

where $J$ is the spectral overlap factor and $V$ is the electronic coupling between D and A, which is assumed to be smaller than $1/KT$. The value of $J$ has been obtained from the experimental spectral overlap between donor emission and acceptor absorption spectra, which have each been normalized to unit area on an energy scale ($J = 280 \times 10^{-6}$ cm in chloroform, $321 \times 10^{-6}$ cm in benzonitrile).

The donor and acceptor units have been constructed by cutting the central C−C bond and capping the unsaturated carbons with hydrogen atoms (see Figure 5).

To take into account the effects of the conformational degrees of freedom of the system, a detailed analysis of the potential energy surface should be performed. However, such an analysis is here extremely expensive due to the large dimensionality of the system and its large conformational flexibility. A simplified strategy has been thus preferred by initially selecting one relevant degree of freedom which is expected to largely affect the mutual orientation between the chromophoric units and their coupling. The selected angle is the dihedral angle $\delta$ defined by the $C_A$, $C_{AD}$, $C_D$, and $N_D$ atoms (see Figure 5). Starting from the fully elongated optimized structure ($\delta = -177°$), we have incremented $\delta$ by multiples of 15 degrees, without reoptimizing the resulting structures, and carried out coupling calculations on these. The EET rates thus obtained, calculated in chloroform using the CAM-B3LYP functional and the 6-311+G(2d,p) basis set, are shown in Figure 6.

As it can be seen from the plot, as expected the EET transfer rate shows a strong dependence on the scanned angle, increasing by several orders of magnitude when moving from the elongated geometry to structures where the D and A units are closer. In particular, two maxima are visible, the highest at $\delta \approx 40°$ and the lowest at $\delta \approx -50°$; these correspond to rate constants of 3.6 and 0.6 $ps^{-1}$, respectively. To better analyze such a strong dependence of the EET rate on the $\delta$ angle, a two-step conformational study was carried out; first, a relaxed scan with


dx.doi.org/10.1021/jp505957q | J. Phys. Chem. C 2014, 118, 23476−23486

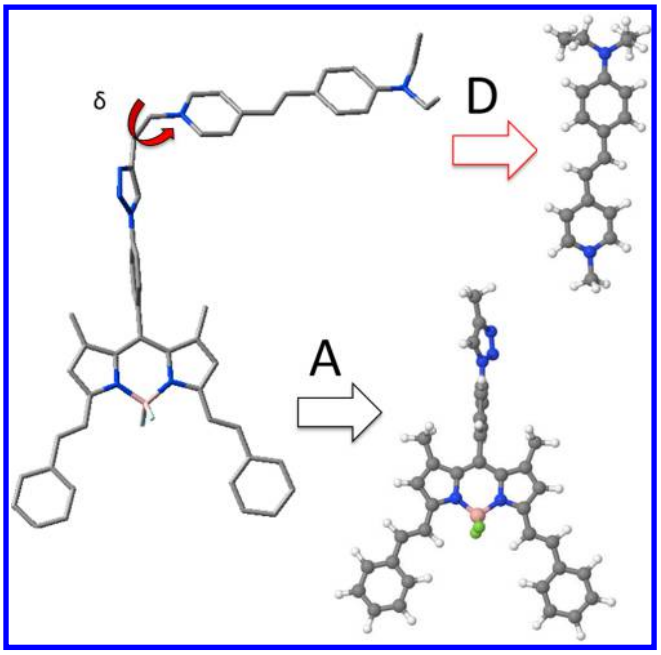


**Figure 5.** Graphical representation of the donor and acceptor units used in the excitonic model.

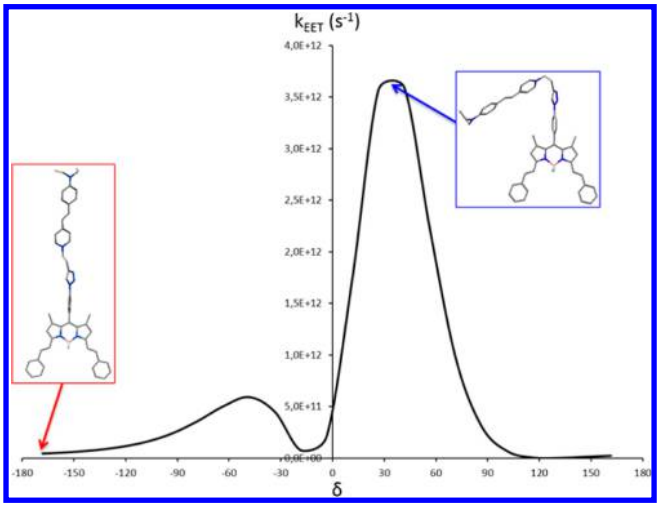


**Figure 6.** Dependence of the EET rate in chloroform on the selected dihedral angle (see Figure 5). Angle values are in degree and $k$ values are in $s^{-1}$.

respect to the $\delta$ angle has been performed, where $\delta$ is constrained to the same set of values used in the previous analysis and the other degrees of freedom are optimized at M06-2x/PCM/6-311G(d) level. Afterward, unconstrained optimizations of the geometry have been performed, starting from selected structures of the scan corresponding to the constrained minima. This study has been repeated for two solvents, chloroform and benzonitrile, and the results are reported in Figure 7.

The behavior of the energy as a function of the angle is similar in the two solvents, showing minima around −180°, −60°, and +60°, the first being quite higher in energy than the other two structures. We note, however, that the dihedral angle $\delta$ only is not sufficient to represent the rotational degrees of freedom between the two chromophoric units which mostly affect their electronic coupling. In particular, a second dihedral angle $\gamma$ defined by the $N_A$, $C_A$, $C_{AD}$, and $C_D$ atoms (see Figure 5) also plays an important

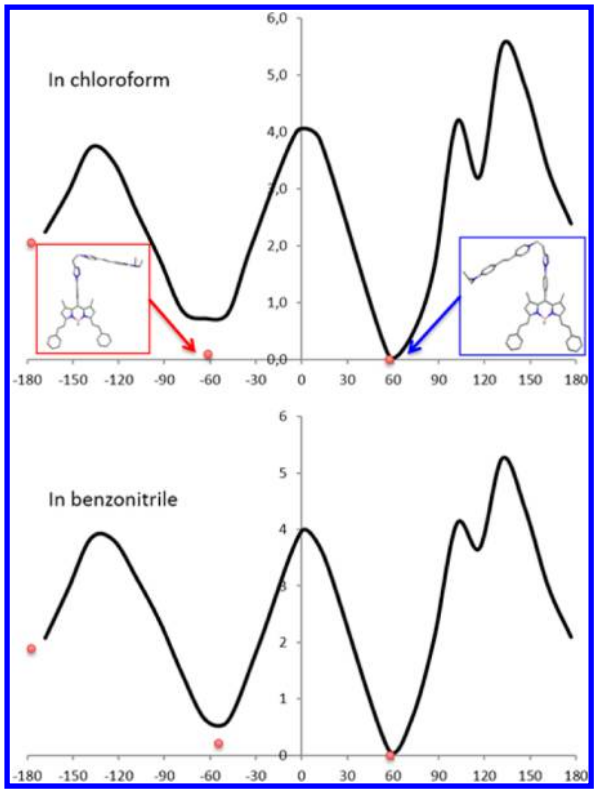


**Figure 7.** Calculated relative energies (in kcal/mol) as a function of the dihedral angles in chloroform (upper panel) and benzonitrile (lower panel). The dots correspond to the fully relaxed geometries obtained starting from the unrelaxed minima. The zero energy corresponds to the absolute minimum in each solvent.

role in tuning the couplings. To have a more complete picture we have refined the previous analysis on $\delta$ with a parallel one on the $\gamma$ angle by finally obtaining that, for chloroform, only two minima are significantly populated, while for benzonitrile three minima are populated (see Table 3). All the minima structures were finally used to calculate the overall EET rate: the obtained results are reported in Table 3. For comparison purposes, in the same table we also report a dipole−dipole approximation of the coupling, as obtained from the transition dipoles computed using the same level of calculation (TD-CAM-B3LYP/6-311+G-(2d,p)).

**Table 3. Calculated Total Coupling $V_{TOT}$ (Including the Solvent Term Reported in eq 2) and EET Times (Calculated As the Inverse of the EET Rate) for the Minima Structures in the Two Solvents[a]**

| | $V_{TOT}$ ($cm^{-1}$) | $t$ (ps) | $R$ (Å) | $V_{Coul}$ ($cm^{-1}$) | $V_{dip\text{-}dip}$ ($cm^{-1}$) |
|---|---|---|---|---|---|
| Chloroform | | | | | |
| $\delta/\gamma$ = 61°/44° (88%) | 79 | 0.48 | 12.5 | 136 | 188 |
| $\delta/\gamma$ = −61°/67° (11%) | 22 | 5.96 | 13.6 | 38 | 115 |
| Benzonitrile | | | | | |
| $\delta/\gamma$ = 58°/55° (6%) | 92 | 0.31 | 12.0 | 175 | 249 |
| $\delta/\gamma$ = −57°/−57° (31%) | 76 | 0.45 | 13.9 | 145 | 317 |
| $\delta/\gamma$ = −54°/83° (63%) | 20 | 6.49 | 13.3 | 39 | 67 |

[a]As a comparison we also report the Coulomb term of the coupling and the corresponding dipole−dipole approximation obtained using the same minima structures and the calculated transition dipoles.


dx.doi.org/10.1021/jp505957q | J. Phys. Chem. C 2014, 118, 23476−23486

As it can be seen from Table 3, the calculations agree well with the experimental findings reported in Table 2, showing two different time scales, one at subpicosecond level and the other of the order of 6 ps. Moreover, if we average the populations obtained in each of the two different solvents we obtain an average time of 1.1 ps in chloroform and 4.2 ps in benzonitrile: once more this result is in agreement with the slower kinetics of energy transfer experimentally observed in benzonitrile. The data reported in Table 3 also show that a dipole−dipole approximation significantly overestimates the Coulomb interaction. However, if we define an effective PCM screening factor as the ratio $(V_{TOT})/V_{Coul}$ we can observe that the screening effect predicted by the $1/n^2$ approximation is also overestimated: for chloroform (benzonitrile) $n$ = 1.446 (1.529) and $1/n^2$ = 0.48 (0.43), while the effective PCM factor is 0.58 (0.52). Therefore, when the dipole−dipole coupling is combined with the $1/n^2$ screening effect, one overestimation roughly compensates the other and the final coupling based on a fully Förster-like approximation becomes close to the TDDFT/PCM estimate.

## DISCUSSION

All the experimental data reported in this work demonstrate that energy transfer in the investigated molecular dyad is highly efficient and largely proceeds on a subpicosecond time scale. In all the examined solvents the kinetics of energy transfer is multiexponential, but at least 70% of the overall process occurs on a subpicosecond time scale. In order to gain insights into the mechanism of this ultrafast energy transfer a theoretical study has been performed, involving both the calculation of the electronic coupling between the donor and acceptor molecular units of the dyad and a conformational analysis of the whole system, based on DFT computations.

Since the experimental absorption spectrum of the dyad suggests the occurrence of weak excitonic coupling between the two units, we have analyzed the kinetics of energy transfer in the frame of the Förster theory. Within this framework,[47] the rate of EET is given by the following equation:

$$K_{EET} = \frac{\phi_D \kappa^2}{\tau_D R^6}\left(\frac{9000\ln(10)}{128\pi^5 N_A n^4}\right)\int_0^\infty \frac{F_D(\nu)\epsilon_A(\nu)}{\nu^4}\,d\upsilon \quad (4)$$

which can be also expressed as

$$K_{EET} = \frac{\phi_D}{\tau_D}\left(\frac{8.785\times 10^{-25} J(\epsilon)}{n^4 R^6}\right) \quad (5)$$

Here $\phi_D$ and $\tau_D$ are the fluorescence quantum yield and lifetime of the donor, $N_A$ is the Avogadro's number, $n$ is the refraction index of the medium, $R$ is the center-to-center separation between the energy donor and acceptor, and $\kappa^2$ is an orientation factor associated with the dipole−dipole interaction between donor and acceptor. The parameters $J(\varepsilon)$ represents the overlap integral between the donor emission $F_D(\nu)$ and the acceptor absorption $\varepsilon_A(\nu)$, expressed in molar extinction coefficient units (liter/mol cm) and in units of frequency in $cm^{-1}$. By inserting into the Förster equation the experimentally evaluated overlap integral, and the measured values of the donor fluorescence quantum yield and lifetime, we find that the subpicosecond energy transfer rate (0.6 ps in chloroform and 0.3 ps in acetonitrile), which accounts for about 70% of the energy transfer, corresponds to a donor−acceptor distance $R$ of about 10 Å. This value is quite close to the calculated distances at the minima structures. This agreement can be explained using the results of the TDDFT calculations of the couplings: although the dipole−dipole approximation implicitly assumed in eq 4 overestimates the real coulomb coupling, such an overestimation is counterbalanced by the parallel overestimation of the solvent screening. Moreover, the TDDFT calculations when combined with the conformational analysis show that, the donor and acceptor units being linked together by means of a saturated covalent bridge, multiple relative orientations are possible with very different couplings. In both less polar and more polar solvents two minimum regions exist on the potential energy surface of the system, where the electronic coupling is relatively larger than that observed in the other conformations, as a result two different time scales of transfer are found. We thus conclude that the rate determining factor for the energy transfer in this system is of conformational nature, that is to say, the energy transfer rate is maximum in those conformations which maximize the coupling value. Moreover, the calculated transfer rate averaged over the different conformations shows a slower kinetics in benzonitrile exactly as observed in the experiments. On the basis of the computational analysis we attribute this findings to a differential stabilization of the minimal structures in the different solvents. In order to further analyze the role of the molecular conformation in determining the energy transfer rate, temperature dependent measurements would be very useful. Also, structural modifications of the donor and acceptor molecules with analogues systems including larger substituents, which would limit the conformational freedom because of the occurrence of steric hindrance, could be taken into account. Finally, solvent effects could also be further analyzed for example by investigating the role of the polarizability: among the analyzed media we in fact observe an inverse trend with the increasing polarizability, since the EET rate increases when going from the most polarizable benzonitrile to the less polarizable of the analyzed solvents, acetonitrile. In any case, although the energy transfer rate can be partly modulated by the external medium, the yield of the process remains quantitative in all the analyzed solvents, further confirming the great potentiality of the BODIPY class of molecules if used as constituents of energy storage and transferring devices, such as artificial antenna systems or solar concentrators.

## CONCLUSIONS

We demonstrate the occurrence of quantitative EET in the analyzed molecular dyad. Although EET in this system is extremely fast, the mechanism of the process can be satisfactorily analyzed in the frame of the Förster model, due to the weak excitonic coupling between the D and A moieties of the dyad. The theoretical analysis performed in this study shows that the estimate of the D−A excitonic couplings obtained from the computed transition densities can adequately reproduce the experimental EET rates, while a dipole−dipole approximation of the Coulomb interaction would overestimate the coupling by at least 40%. The conformational analysis of the D−A dyad performed with DFT calculations shows that the system can assume multiple conformations, but two energy minimum regions exists on the potential energy surface for which the D−A electronic coupling has its maximum value. Our study thus demonstrates that the interplay between experimental and theoretical methods can be beneficial in disentangling which molecular factors play a prominent role in determining the efficiency and dynamics of energy transfer in simple donor−acceptor systems.


dx.doi.org/10.1021/jp505957q | J. Phys. Chem. C 2014, 118, 23476−23486

## ■ ASSOCIATED CONTENT

### Supporting Information

Additional time-resolved spectra in acetonitrile and benzonitrile. This material is available free of charge via the Internet at http://pubs.acs.org.

## ■ AUTHOR INFORMATION


### Corresponding Author

*E-mail: didonato@lens.unifi.it.


### Notes

The authors declare no competing financial interest.

## ■ ACKNOWLEDGMENTS

The authors gratefully acknowledge support from the Italian MIUR: program FIRB "Futuro in Ricerca 2010" grant RBFR10Y5VW to M.D.D. and RBFR109ZHQ supporting A.L., project EFOR-CABIR L. 191/2009 art. 2 comma 44, and grant FIRB RBAP11ETKA_002 'Approcci nanotecnologici per la teragnostica dei tumori' to S. Cicchi. B.M. and S. Caprasecca thank the ERC for financial support in the framework of the Starting Grant (EnLight -277755).

## ■ REFERENCES


(1) Balzani, V.; Credi, A.; Venturi, M. Photochemical Conversion of Solar Energy. *ChemSusChem* **2008**, *1*, 26−58.

(2) Gust, D.; Moore, T. A.; Moore, A. L. Solar Fuels via Artificial Photosynthesis. *Acc. Chem. Res.* **2009**, *42*, 1890−1898.

(3) Barber, J. Photosynthetic Energy Conversion: Natural and Artificial. *Chem. Soc. Rev.* **2009**, *38*, 185−196.

(4) Scholes, G. D.; Fleming, G. R.; Olaya-Castro, A.; van Grondelle, R. Lessons from Nature about Solar Light harvesting. *Nat. Chem.* **2011**, *3*, 763−744.

(5) McConnell, I.; Li, G.; Brudvig, G. W., Energy Conversion in Natural and Artificial Photosynthesis. *Chem. Biol. 17*, 434−447.

(6) *The Photosynthetic Reaction Center*; Deisenhofer, J., Norris, J. R., Eds.; Academic Press: New York, 1993.

(7) *Molecular Mechanism of Photosynthesis*. Blankeship, R.E., Ed.; Blackwell Science: Oxford, 2002.

(8) Sabatini, R. P.; McCormick, T. M.; Lazarides, T.; Wilson, K. C.; Eisenberg, R.; McCamant, D. W. Intersystem Crossing in Halogenated Bodipy Chromophores Used for Solar Hydrogen Production. *J. Phys. Chem. Lett.* **2011**, *2*, 223−227.

(9) Bai, D.; Benniston, A. C.; Hagon, J.; Lemmetyinen, H.; Tkachenko, N. V.; Harrington, R. W. Tuning the Forster Overlap Integral: Energy Transfer over 20 Angstroms from a Pyrene-Based Donor to Borondipyrromethene (Bodipy). *Phys. Chem. Chem. Phys.* **2013**, *15*, 9854−9861.

(10) El-Khouly, M. E.; Fukuzumi, S.; D'Souza, F. Photosynthetic Antenna−Reaction Center Mimicry by Using Boron Dipyrromethene Sensitizers. *ChemPhysChem* **2014**, *15*, 30−47.

(11) Shi, W.-J.; El-Khouly, M. E.; Ohkubo, K.; Fukuzumi, S.; Ng, D. K. P. Photosynthetic Antenna-Reaction Center Mimicry with a Covalently Linked Monostyryl Boron-Dipyrromethene−Aza-Boron-Dipyrromethene−C60 Triad. *Chem.—Eur. J.* **2013**, *19*, 11332−11341.

(12) D'Souza, F.; Smith, P. M.; Zandler, M. E.; McCarty, A. L.; Itou, M.; Araki, Y.; Ito, O. Energy Transfer Followed by Electron Transfer in a Supramolecular Triad Composed of Boron Dipyrrin, Zinc Porphyrin, and Fullerene: A Model for the Photosynthetic Antenna-Reaction Center Complex. *J. Am. Chem. Soc.* **2004**, *126*, 7898−7907.

(13) Guo, S.; Ma, L.; Zhao, J.; Kucukoz, B.; Karatay, A.; Hayvali, M.; Yaglioglu, H. G.; Elmali, A. BODIPY Triads Triplet Photosensitizers Enhanced with Intramolecular Resonance Energy Transfer (RET): Broadband Visible Light Absorption and Application in Photooxidation. *Chem. Sci.* **2014**, *5*, 489−500.

(14) Loudet, A.; Burgess, K. BODIPY Dyes and Their Derivatives: Syntheses and Spectroscopic Properties. *Chem. Rev.* **2007**, *107*, 4891−4932.

(15) Narang, U.; Zhao, C. F.; Bhawalkar, J. D.; Bright, F. V.; Prasad, P. N. Characterization of a New Solvent-Sensitive Two-Photon-Induced Fluorescent (Aminostyryl)pyridinium Salt Dye. *J. Phys. Chem.* **1996**, *100*, 4521−4525.

(16) Zhao, C. F.; Gvishi, R.; Narang, U.; Ruland, G.; Prasad, P. N. Structures, Spectra, and Lasing Properties of New (Aminostyryl)-pyridinium Laser Dyes. *J. Phys. Chem.* **1996**, *100*, 4526−4532.

(17) Mishra, A.; Behera, P. K.; Behera, R. K.; Mishra, B. K.; Behera, G. B. Interaction of N-alkyl Styryl Pyridinium Dyes with TX-100 in Aqueous Medium: Role of the Alkyl Chain During Solubilisation. *J. Photochem. Photobiol. A* **1998**, *116* (1), 79−84.

(18) van der Meer, M. J.; Zhang, H.; Rettig, W.; Glasbeek, M. Femto- and Picosecond Fluorescence Studies of Solvation and Non-Radiative Deactivation of Ionic Styryl Dyes in Liquid Solution. *Chem. Phys. Lett.* **2000**, *320*, 673−680.

(19) Mishra, A.; Behera, G. B.; Krishna, M. M. G.; Periasamy, N. Time-Resolved Fluorescence Studies of Aminostyryl Pyridinium Dyes in Organic Solvents and Surfactant Solutions. *J. Lumin.* **2001**, *92*, 175−188.

(20) Forster, T. 10th Spiers Memorial Lecture. Transfer Mechanisms of Electronic Excitation. *Discuss. Faraday Soc.* **1959**, *27*, 7−17.

(21) Langille, N. F.; Jamison, T. F. trans-Hydroalumination/Alkylation: One-Pot Synthesis of Trisubstituted Allylic Alcohols. *Org. Lett.* **2006**, *8*, 3761−3764.

(22) Fischer, M.; Georges, J. Fluorescence Quantum Yield of Rhodamine 6G in Ethanol as a Function of Concentration Using Thermal Lens Spectrometry. *Chem. Phys. Lett.* **1996**, *260*, 115−118.

(23) Sens, R. d.; Drexhage, K. H. Fluorescence Quantum Yield of Oxazine and Carbazine Laser Dyes. *J. Lumin.* **1981**, *24*, 709−712.

(24) Darses, B.; Michaelides, I. N.; Sladojevich, F.; Ward, J. W.; Rzepa, P. R.; Dixon, D. J. Expedient Construction of the [7−5-5] All-Carbon Tricyclic Core of the Daphniphyllum Alkaloids Daphnilongeranin B and Daphniyunnine D. *Org. Lett.* **2012**, *14*, 1684−1687.

(25) Facchetti, A.; Abbotto, A.; Beverina, L.; van der Boom, M. E.; Dutta, P.; Evmenenko, G.; Pagani, G. A.; Marks, T. J. Layer-by-Layer Self-Assembled Pyrrole-Based Donor-Acceptor Chromophores as Electro-Optic Materials. *Chem. Mater.* **2003**, *15*, 1064−1072.

(26) Maligaspe, E.; Tkachenko, N. V.; Subbaiyan, N. K.; Chitta, R.; Zandler, M. E.; Lemmetyinen, H.; D'Souza, F. Photosynthetic Antenna-Reaction Center Mimicry: Sequential Energy- and Electron Transfer in a Self-assembled Supramolecular Triad Composed of Boron Dipyrrin, Zinc Porphyrin and Fullerene. *J. Phys. Chem. A* **2009**, *113*, 8478−8489.

(27) Lu, H.; Zhang, S.; Liu, H.; Wang, Y.; Shen, Z.; Liu, C.; You, X. Experimentation and Theoretic Calculation of a BODIPY Sensor Based on Photoinduced Electron Transfer for Ions Detection. *J. Phys. Chem. A* **2009**, *113*, 14081−14086.

(28) Jose, J.; Ueno, Y.; Castro, J. C.; Li, L.; Burgess, K. Energy Transfer Dyads Based on Nile Red. *Tetrahedron Lett.* **2009**, *50*, 6442−6445.

(29) Marcelli, A.; Foggi, P.; Moroni, L.; Gellini, C.; Salvi, P. R. Excited-State Absorption and Ultrafast Relaxation Dynamics of Porphyrin, Diprotonated Porphyrin, and Tetraoxaporphyrin Dication. *J. Phys. Chem. A* **2008**, *112*, 1864−1872.

(30) Gentili, P. L.; Mugnai, M.; Bussotti, L.; Righini, R.; Foggi, P.; Cicchi, S.; Ghini, G.; Viviani, S.; Brandi, A. The Ultrafast Energy Transfer Process in Naphtol-Nitrobenzofurazan Bichromophoric Molecular Systems: A Study by Femtosecond UV-vis Pump-Probe Spectroscopy. *J. Photochem. Photobiol. A* **2007**, *187*, 209−221.

(31) Gentili, P. L.; Bussotti, L.; Ruzziconi, R.; Spizzichino, S.; Foggi, P. Study of the Photobehavior of a Newly Synthesized Chiroptical Molecule: (E)-(Rp,Rp)-1,2-Bis{4-methyl[2]paracyclo[2](5,8)-quinolinophan-2-yl}ethene. *J. Phys. Chem. A* **2009**, *113*, 14650−14656.

(32) Moroni, L.; Gellini, C.; Salvi, P. R.; Marcelli, A.; Foggi, P. Excited States of Porphyrin Macrocycles. *J. Phys. Chem. A* **2008**, *112*, 11044−11051.

(33) Bayanov, I. M.; Danielius, R.; Heinz, P.; Seilmeier, A. Intense Subpicosecond Pulses Tunable Between 4$\mu$m and 20 $\mu$m Generated by an All-Solid-State Laser System. *Opt. Commun.* **1994**, *113*, 99−104.

(34) Danielius, R.; Piskarskas, A.; Di Trapani, P.; Andreoni, A.; Solcia, C.; Foggi, P. Visible Pulses of 100 fs and 100 $\mu$J from an Upconverted Parametric Generator. *Appl. Opt.* **1996**, *35*, 5336−5339.
(35) Henry, E. R. The Use of Matrix Methods in the Modeling of Spectroscopic Data Sets. *Biophys. J.* **1997**, *72*, 652−673.
(36) Henry, E. R.; Hofrichter, J. [8] Singular value decomposition: Application to analysis of experimental data. *Meth. Enzymol.* **1992**, *210*, 129−192.
(37) van Stokkum, I. H. M.; Larsen, D. S.; van Grondelle, R. Global and Target Analysis of Time-Resolved Spectra. *BBA - Bioenerg.* **2004**, *1657*, 82−104.
(38) Snellenburg, J. J.; Laptenok, S. P.; Seger, R.; Mullen, K. M.; van Stokkum, I. H. M. Glotaran: A Java -Based Graphical User Interface for the R Package TIMP. *J. Stat. Soft.* **2012**, *49*, 1−22.
(39) Mullen, K. M.; van Stokkum, I. H. M. An Introduction to the Special Volume "Spectroscopy and Chemometrics in R. *J. Stat. Soft.* **2007**, *18*, 1−5.
(40) Tomasi, J.; Mennucci, B.; Cammi, R. Quantum Mechanical Continuum Solvation Models. *Chem. Rev.* **2005**, *105*, 2999−3094.
(41) Hsu, C.-P.; Fleming, G. R.; Head-Gordon, M.; Head-Gordon, T. Excitation Energy Transfer in Condensed Media. *J. Chem. Phys.* **2001**, *114*, 3065−3072.
(42) Iozzi, M. F.; Mennucci, B.; Tomasi, J.; Cammi, R. Excitation Energy Transfer (EET) Between Molecules in Condensed Matter: A Novel Application of the Polarizable Continuum Model (PCM). *J. Chem. Phys.* **2004**, *120*, 7029−7040.
(43) Frisch, M. J.; et al. *Gaussian 09,* revision D.01; Gaussian, Inc.: Wallingford, CT, 2009.
(44) Zhao, Y.; Truhlar, D. The M06 Suite of Density Functionals for Main Group Thermochemistry, Thermochemical Kinetics, Noncovalent Interactions, Excited States, and Transition Elements: Two New Functionals and Systematic Testing of Four M06-Class Functionals and 12 Other Functionals. *Theor. Chem. Acc.* **2008**, *120*, 215−241.
(45) Yanai, T.; Tew, D. P.; Handy, N. C. A New Hybrid Exchange and Correlation Functional Using the Coulomb-Attenuating Method (CAM-B3LYP). *Chem. Phys. Lett.* **2004**, *393*, 51−57.
(46) Cancès, E.; Mennucci, B.; Tomasi, J. A New Integral Equation Formalism for the Polarizable Continuum Model: Theoretical Background and Applications to Isotropic and Anisotropic Dielectrics. *J. Chem. Phys.* **1997**, *107*, 3032−3041.
(47) Scholes, G. D. Long-Range Energy transfer in Molecular Systems. *Annu. Rev. Phys. Chem.* **2003**, *54*, 57−87.